

Cluster Prediction for Opinion Dynamics from Partial Observations

Zehong Zhang, and Fei Lu

Abstract—We present a Bayesian approach to predict the clustering of opinions for a system of interacting agents from partial observations. The Bayesian formulation overcomes the unobservability of the system and quantifies the uncertainty in the prediction. We characterize the clustering by the posterior of the clusters’ sizes and centers, and we represent the posterior by samples. To overcome the challenge in sampling the high-dimensional posterior, we introduce an auxiliary implicit sampling (AIS) algorithm using two-step observations. Numerical results show that the AIS algorithm leads to accurate predictions of the sizes and centers for the leading clusters, in both cases of noiseless and noisy observations. In particular, the centers are predicted with high success rates, but the sizes exhibit a considerable uncertainty that is sensitive to observation noise and the observation ratio.

Index Terms—Clustering prediction, opinion dynamics, Bayesian approach, state space model, sequential Monte Carlo

I. INTRODUCTION

CLUSTERING behavior in a network of interacting agents or particles arises in a vast range of disciplines [1]–[3]. In the context of opinion dynamics of social networks, local interactions among agents cause opinions to evolve, formulating one or more clusters of opinions. While the striking phenomenon of consensus (one cluster) has attracted long-standing interest, non-consensus clustering, in which multiple stable clusters coexist, has attracted increasing interest to resemble the real-life social network [4]–[7]. Such clustering of opinions or communities have a profound impact on the network, so it is of great importance to predict these clusters from observations, which are often partial, at an early stage.

We investigate the prediction of clusters for multi-agent opinion dynamics with multiple clusters, from short-time partial observations which may be contaminated by noise. In particular, our objective is to predict the sizes and centers of the leading clusters. We assume the system is known (we refer to [8]–[10] and the references therein for the learning of the governing equation from data). To predict the clustering, one may estimate all agents’ current opinions and use them as an initial configuration for prediction. However, we show that it is an ill-posed inverse problem to estimate the current state from partial observations (widely-studied as observability in control, see e.g., [11]). We propose a Bayesian formulation to make the problem well-posed: we estimate the posterior distribution of the states conditional on the observations. We represent the posterior by samples, which provide initial configurations for

prediction. This procedure yields a posterior for the clusters’ sizes and centers, quantifying the uncertainty in prediction.

The major challenge in the Bayesian approach is to generate samples for the high-dimensional posterior. Due to the intrinsic symmetry of the nonlinear opinion dynamics, the non-Gaussian posterior has multiple local extrema, which posed a hurdle for the performance of Sequential Monte Carlo (SMC) methods [12]–[14], including the optimal (one-step-observation) importance sampling methods such as implicit sampling [15]. The symmetry between the agents also prevents the feedback control or nudging methods [16]–[22] based on dominating modes in the observation.

We overcome the challenge by introducing an Auxiliary Implicit Sampling (AIS) algorithm that makes use of two-step observations, which is a sequential Monte Carlo method that combines the ideas from auxiliary particle filters [23], implicit sampling [15] and feedback control [20]. We also introduce an MCMC-move step to reduce sample degeneracy and an information move step to reject non-physical samples.

Numerical tests show that our AIS algorithm leads to accurate prediction of the sizes and centers for the leading clusters, in both cases of noiseless and noisy observations. In particular, the centers of the leading clusters are predicted with a high success rate, but the size of the leading cluster exhibits a considerable uncertainty that is sensitive to observation noise and the observation ratio. Our AIS algorithm brings improvement to implicit sampling, and both outperform the sequential importance sampling with resampling (SIR) method.

The exposition in our manuscript proceeds as follows. In Section II, we define clusters for opinion dynamics with local interactions, prove that the inverse problem of state estimation from partial observation is ill-posed, and propose a Bayesian formulation for cluster prediction. To represent the posterior, we introduce in Section III an auxiliary implicit sampling algorithm that designs importance densities based on two-step observations. Section IV examines the performance of the AIS algorithm in numerical simulations. Finally, Section V concludes the paper with discussions.

II. BAYESIAN APPROACH TO CLUSTER PREDICTION

Consider a group of N agents, each with an opinion at time t quantified by $x_t^i \in \mathbb{R}^d$, interacting with each other according to a first-order difference system:

$$x_{t+1}^i - x_t^i = \frac{\alpha}{N} \sum_{j=1}^N \phi(\|x_t^j - x_t^i\|)(x_t^j - x_t^i). \quad (1)$$

Here, the positive constant α is a scaling parameter and the interaction kernel ϕ is a non-negative function supported on

$[0, R]$. The agents interact locally, only with those opinions that are “close” in the sense that the pairwise distance $\|x_t^i - x_t^j\|$ is less than R , with the strength of interaction the kernel.

Our goal is to predict the clustering of the system, particularly the sizes and the centers of the leading clusters, supposing that we only observe the trajectories of N_1 of the N agents for a relatively short time, far before the system forms clusters.

In this section, we provide a quantitative definition for clustering and discuss clustering prediction from partial observations. We show that it is an ill-posed inverse problem to predict the clustering by estimating all agents’ trajectories. We introduce a Bayesian approach to make the problem well-posed, providing a probabilistic quantification of the uncertainty in the prediction.

A. Definition of clusters

Due to the local interaction between agents, clusters of opinions will emerge, in which each agent only interacts with agents within the same cluster. More precisely, we define the system is in a clustered status as follows:

Definition 1 (Clustered status): Let $x_t \in \mathbb{R}^{dN}$ be the state of the system (1) with a local interaction kernel ϕ supported on $[0, R]$. We say the system is **clustered** if the index set $\{1, 2, \dots, N\}$ of agents can be partitioned into disjoint clusters $\mathcal{C}_1(t), \dots, \mathcal{C}_m(t)$ such that for any $i \in \mathcal{C}_{k_1}(t)$ and $j \in \mathcal{C}_{k_2}(t)$:

- (i) if $k_1 = k_2$, then $\|x_t^i - x_t^j\| < R$,
- (ii) if $k_1 \neq k_2$, then $\|x_t^i - x_t^j\| > R$.

An essential feature of the clustered status is that it is invariant in time: a clustered system will remain clustered with the same clusters. In particular, each cluster is isolated from other clusters; in each cluster, the agents formulate a self-contained dynamics and concentrate towards a local consensus, the center of the cluster, since the interaction is symmetric (we refer to [3] for detailed discussions on clustering for local interactions). We summarize this invariant feature as a property of the system.

Property 1 (Invariants of a clustered system): Suppose that at time t_c , the system (1) is clustered into $\{\mathcal{C}_1, \dots, \mathcal{C}_K\}$. Then, the system will remain clustered with the same clusters for all $t \geq t_c$. In particular, the sizes and the centers of the clusters are invariant in time: for all $t \geq t_c$,

$$\begin{aligned} |\mathcal{C}_k| &:= |\mathcal{C}_k(t)| = |\mathcal{C}_k(t_c)|, \\ \bar{x}_{\mathcal{C}_k} &:= \frac{1}{|\mathcal{C}_k(t)|} \sum_{i \in \mathcal{C}_k(t)} x_t^i = \frac{1}{|\mathcal{C}_k(t_c)|} \sum_{i \in \mathcal{C}_k(t_c)} x_{t_c}^i. \end{aligned} \quad (2)$$

for each $k = 1, \dots, K$, where $|\mathcal{C}_k|$ and $\bar{x}_{\mathcal{C}_k}$ denote the size (number of agents) and center (mean opinion of agents) of cluster \mathcal{C}_k , respectively.

These invariants characterize the clustering (the large time behavior) of the opinion system. Therefore, our goal of clustering prediction is to estimate these invariants: the sizes and centers of the clusters, particularly those of the largest clusters.

B. Cluster identification from partial observations

In practice, it is often the case that we can only observe or track partial of the agents. We consider the case that

TABLE 1
Notation of variables in the state-space model

Notation	Description
$x = (x^1, \dots, x^N) \in \mathbb{R}^{dN}$	state variable of the system
$Hx = (x^1, \dots, x^{N_1}), H_i x = x^i$	opinions of observed agents
$Gx = (x^{N_1+1}, \dots, x^N)$	opinions of unobserved agents
$ \mathcal{C}_i $ and $\bar{x}_{\mathcal{C}_i}$	size and center of cluster \mathcal{C}_i
$x_{1:t} = (x_1, \dots, x_t) \in \mathbb{R}^{tdN}$	trajectory of all agents
$z_{1:t} = (z_1, \dots, z_t) \in \mathbb{R}^{tdN_1}$	trajectory of observed agents

N_1 out of the N agents are observed, with $z_{1:T} \in \mathbb{R}^{TdN_1}$ denoting their trajectories. We will consider either noiseless or noisy observations. The original model (1), together with an observation equation, can be written as the following state space model:

$$\begin{cases} x_{t+1} = g(x_t), \\ z_t = Hx_t + \xi_t, \end{cases} \quad (3)$$

where $g(x_t)$ is the right-hand-side of (1), and $H : \mathbb{R}^{dN} \rightarrow \mathbb{R}^{dN_1}$ is a projection operator mapping the vector of opinions of all agents to its observed part. Without loss of generality, we assume that the first N_1 agents are observed. For simplicity of notation, we denote $Hx = (x^1, \dots, x^{N_1}) \in \mathbb{R}^{dN_1}$ with $H = [I_{dN_1} \mid 0 \times I_{dN_2}]$ and with $H_i x = x^i$ as the i -th observed agent. Similarly, for the unobserved agents, we define projection operator $G : \mathbb{R}^{dN} \rightarrow \mathbb{R}^{dN_2}$ from the state x to its unobserved part, denoting $Gx = (x^{N_1+1}, \dots, x^N) \in \mathbb{R}^{dN_2}$ with $G = [0 \times I_{dN_1} \mid I_{dN_2}]$ and with $G_i x = x^{N_1+i}$ as the i -th unobserved agent. We summarize the notation in Table 1.

To predict the clustering, which is the large time behavior of the dynamics, based on observations up to time T , a natural idea is to (i) estimate the state of the system at time T , and (ii) use the estimated state as an initial condition for a long time simulation until the system is clustered. For Step (i), one may wish to find a trajectory of the state variable that fits the observation data. However, the following section shows that even with noiseless partial observations, it is an ill-posed inverse problem to identify the trajectory $x_{1:T}$ from observation $z_{1:T}$. Also, whereas a regularization can make the problem well-posed in a variational approach, it leads to a challenging high-dimensional optimization problem on the path space and there may be many local minima caused by the symmetry of the system. Instead, we adopt a Bayesian approach that avoids high-dimensional optimization and quantifies the uncertainty in prediction.

C. State estimation and observability

In general, it is an ill-posed inverse problem to estimate the trajectory of all agents from partial noiseless observations. We demonstrate this by an example of symmetric trajectories and by proving that the unobserved trajectories can not be uniquely determined in linear systems, referred to as unobservability in control (see e.g., [11]), when more than one agents are unobserved.

The next example shows that as long as more than two agents are unobserved, there could be symmetric trajectories, making it an ill-posed problem to identify the trajectories.

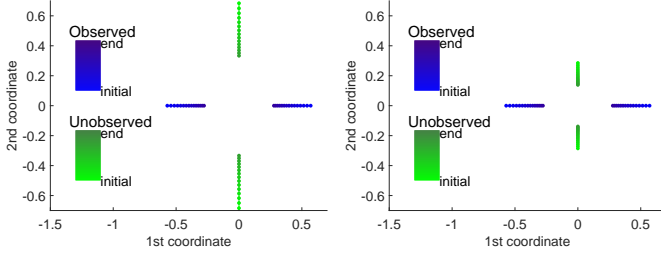


Fig. 1: Illustration of symmetric trajectories: same observed trajectories (blue points) are generated from different configurations (with different unobserved trajectories in green). The color changes from light to dark to indicate time increasing from initial to end-time of observation.

Example 1 (Symmetric trajectories): Consider a system with $N = 4$ agents in \mathbb{R}^2 and suppose that we observe $N_1 = 2$ of them. Figure 1 illustrates that two different configurations can lead to the same observations. The symmetric positions of the two unobserved agents canceled out their different influence on the observed agents.

The following theorem show that it is an ill-posed problem to estimate the states of the system when more than one agents is unobserved in the case of linear systems.

Theorem 1 (Observability for linear opinion dynamics): Consider the linear dynamics with $\phi \equiv 1$ in (1), and suppose that we observed the trajectory of N_1 agents. Then, the trajectories of the unobserved agents can be uniquely determined if and only if

$$N_1 \geq N - 1.$$

Proof 1: We only need to consider $N_1 \leq N - 1$. We can write the system as

$$\begin{cases} x_{t+1} = \alpha A x_t + x_t, \\ z_t = H x_t, \end{cases}$$

where $A \in \mathbb{R}^{dN} \times \mathbb{R}^{dN}$ is a constant matrix,

$$A = \begin{pmatrix} c_1 I_d & c_2 I_d & \cdots & c_2 I_d \\ c_2 I_d & c_1 I_d & \cdots & c_2 I_d \\ \vdots & \vdots & \ddots & \vdots \\ c_2 I_d & c_2 I_d & \cdots & c_1 I_d \end{pmatrix}$$

with $c_1 = -\frac{(N-1)}{N}$ and $c_2 = \frac{1}{N}$. By the observability theory [11], the trajectory $x_{1:T}$ can be uniquely determined from the observations $z_{1:T}$ if and only if $\text{rank}(W) = dN$, where

$$W := [H^T \mid A^T H^T \mid \dots \mid (A^T)^{n-1} H^T].$$

To compute $\text{rank}(W)$, note that $A^T = A$ and $A = Q\Lambda Q^T$, where $\Lambda = \text{diag}(-I_{d(N-1)}, 0 \times I_d)$ and Q is a unitary matrix. Recalling that $H = [I_{dN_1} \mid 0 \times I_{dN_2}]$, we have $(A^T)^k H^T = (-1)^{k-1} A H^T$ for $k = 1, \dots, n-1$. Thus,

$$\text{rank}(W) = \text{rank}([H^T \mid A H^T]) = (N_1 + 1) \times d.$$

D. Bayesian estimation of states and clusters

In a Bayesian approach, we view the states and the invariants of the clusters as random variables and we aim to represent their posteriors conditional on the observations.

TABLE 2
Notation of variables in the Bayesian approach

Notation	Description
$p(x_{1:T} \mid z_{1:T})$,	posterior of $x_{1:T}$ conditional on $z_{1:T}$
$\hat{p}(x_{1:T} \mid z_{1:T})$	empirical approximation of $p(x_{1:T} \mid z_{1:T})$
$\{x_{1:t}^{(s)}, w_t^{(s)}\}$	samples and weights
$p(\mathcal{C}_i \mid z_{1:T})$, $p(\bar{x}_{\mathcal{C}_i} \mid z_{1:T})$	posteriors of $ \mathcal{C}_i $ and $\bar{x}_{\mathcal{C}_i}$

We begin by writing the system in the form of a state space model:

$$\begin{cases} x_{t+1} = g(x_t) + \epsilon_t, & x_1 \sim \mu(\cdot), \\ z_t = H x_t + \xi_t, \end{cases} \quad (4)$$

where the state-noise ϵ_t and observation-noise ξ_t are 0 in the noiseless case. When these two noise terms are zero, the randomness of the states comes from the initial distribution μ . Conditional on observations $z_{1:T}$, we denote by $p(|\mathcal{C}_i| \mid z_{1:T})$, and $p(\bar{x}_{\mathcal{C}_i} \mid z_{1:T})$ the posteriors of the size and center of cluster \mathcal{C}_i , and similarly for the state variables, as in Table 2.

These posteriors of the invariants depend on the initial distribution as well as the system, and can not be expressed analytically in general. They depend on the posterior of the state $p(x_{1:T} \mid z_{1:T})$, particularly $p(x_T \mid z_{1:T})$ when the opinion dynamics is deterministic. The analytical expression of these posteriors of the state variables may be available, but they are high-dimensional and non-Gaussian.

We approximate these distributions by Monte-Carlo methods: we draw a set of weighted samples (with normalized weights), $\{x_{1:t}^{(s)}, w_t^{(s)}\}_{s \in \{1, \dots, S\}}$, by a sequential Monte Carlo method (to be introduced in the next section) from the target distribution $p(x_{1:T} \mid z_{1:T})$, and obtain empirical approximations of these distributions. For instance, the posterior $p(x_T \mid z_{1:T})$ is approximated by

$$\hat{p}(x_T \mid z_{1:T}) = \sum_{s=1}^S w_T^{(s)} \delta_{x_T^{(s)}}(x).$$

By running the original system from each of the samples $\{x_T^{(s)}\}$ until the status of clustered, we obtain weighted samples for the invariance of clusters $\{\bar{x}_{\mathcal{C}_i}^{(s)}, w_T^{(s)}\}_{s \in \{1, \dots, S\}}$ and $\{|\mathcal{C}_i^{(s)}|, w_T^{(s)}\}_{s \in \{1, \dots, S\}}$. With these weighted samples, we have the empirical posterior to quantify the uncertainty in cluster prediction:

$$\begin{cases} \hat{p}(\bar{x}_{\mathcal{C}_i} \mid z_{1:T}) = \sum_{s=1}^S w_T^{(s)} \delta_{\bar{x}_{\mathcal{C}_i}^{(s)}}(\bar{x}_{\mathcal{C}_i}), \\ \hat{p}(|\mathcal{C}_i| \mid z_{1:T}) = \sum_{s=1}^S w_T^{(s)} \delta_{|\mathcal{C}_i^{(s)}|}(|\mathcal{C}_i|). \end{cases} \quad (5)$$

With the weighted sample, we can efficiently approximate statistics by the samples. For example, the expectations of the size and center of cluster \mathcal{C}_i are

$$\begin{aligned} \mathbb{E}(\bar{x}_{\mathcal{C}_i}) &\approx \widehat{\bar{x}_{\mathcal{C}_i}} := \sum_{s=1}^S \bar{x}_{\mathcal{C}_i}^{(s)} \cdot w_T^{(s)}, \\ \mathbb{E}(|\mathcal{C}_i|) &\approx \widehat{|\mathcal{C}_i|} := \sum_{s=1}^S |\mathcal{C}_i^{(s)}| \cdot w_T^{(s)}. \end{aligned} \quad (6)$$

III. SAMPLING THE POSTERIOR

To initiate the ensemble simulation for prediction, we draw samples from the conditional distribution of the current state, $p(x_T | z_{1:T})$, which is the marginal distribution of the posterior distribution $p(x_{1:T} | z_{1:T})$. This posterior is high-dimensional, nonlinear and non-Gaussian, therefore it is difficult to sample directly, even when its analytical form is explicitly available.

We will adopt a Sequential Monte Carlo (SMC) strategy (we refer to [12] for a review), with a combination of implicit sampling [15] and Auxiliary particle filtering, and some specialized MCMC-move and information-move.

To avoid degenerate distributions, we introduce noises to the state-space model (4) from section II-D by setting the noises ϵ_t and ξ_t to be i.i.d. Gaussian,

$$\begin{cases} x_{t+1} = g(x_t) + \epsilon_t, & x_1 \sim \mu(\cdot), \\ z_t = Hx_t + \xi_t. \end{cases}$$

A. Sequential Monte Carlo sampling

The SMC methods, or particle filters, are a set of sequential importance sampling algorithms that approximates the high dimensional distribution $p(x_{1:t} | z_{1:t})$ by its empirical distribution from weighted samples $\{x_{1:t}^{(s)}, w_t^{(s)}\}_{s \in \{1, \dots, S\}}$:

$$\hat{p}(x_{1:t} | z_{1:t}) := \frac{1}{\sum_{s=1}^S w_t^{(s)}} \sum_{s=1}^S w_t^{(s)} \delta_{x_{1:t}^{(s)}}(x),$$

where δ is Dirac delta mass. The samples $\{x_{1:t}^{(s)}\}$ are drawn from an importance distribution $q(x_{1:t} | z_{1:t})$ and the weights are computed from

$$w(x_{1:t} | z_{1:t}) = \frac{p(x_{1:t} | z_{1:t})}{q(x_{1:t} | z_{1:t})}. \quad (7)$$

The key idea of SMC is to generate the weighted samples sequentially from a recursive importance density,

$$q(x_{1:t} | z_{1:t}) = q(x_1) \prod_{k=2}^t q(x_k | x_{1:k-1}, z_{1:k}), \quad (8)$$

which is constructed based on the recursive representation of the posterior distribution:

$$p(x_{1:t} | z_{1:t}) = p(x_{1:t-1} | z_{1:t-1}) \frac{p(x_t | x_{t-1}) p(z_t | x_t)}{p(z_t | z_{1:t-1})}, \quad (9)$$

That is, at time t , conditional on previous samples $\{x_{1:t-1}^{(s)}, w_{t-1}^{(s)}\}_{s \in \{1, \dots, S\}}$, one generates weighted samples $\{x_t^{(s)}\}$ from importance densities $\{q(x_t | x_{1:t-1}^{(s)}, z_{1:t})\}$ and compute their weights by

$$w_t^{(s)} = w_{t-1}^{(s)} \cdot \frac{p(z_t | x_t^{(s)}) \cdot p(x_t^{(s)} | x_{t-1}^{(s)})}{q(x_t^{(s)} | x_{1:t-1}^{(s)}, z_{1:t})}. \quad (10)$$

Clearly, the above weight $w_t^{(s)}$ is proportional to the analytical weight $w(x_{1:t}^{(s)} | z_{1:t})$ since $p(x_{1:t}^{(s)} | z_{1:t}) \propto p(x_{1:t-1}^{(s)} | z_{1:t-1}) \cdot p(x_t^{(s)} | x_{t-1}^{(s)}) p(z_t | x_t^{(s)})$ and $q(x_{1:t}^{(s)} | z_{1:t-1}) = q(x_{1:t-1}^{(s)} | z_{1:t-1}) \cdot q(x_t^{(s)} | x_{1:t-1}^{(s)}, z_{1:t})$.

Due to the recursive computation in (10), all but a few of the weights will be almost zero as t increases, and this is

called sample degeneracy [12]. As a result, the variance of our estimation $\{x_t^{(s)}\}$ may increase exponentially with t (see e.g. [24]). Resampling techniques are widely used to reduce sample degeneracy: it replaces samples with relatively low weights by samples with relatively high weights. A simple resampling technique is to define effective sample size (ESS) [25] by $\text{ESS}_t = (\sum_{i=1}^S w_t^{(i)})^2 / (\sum_{i=1}^S (w_t^{(i)})^2)$. If at time t , ESS_t reaches below a threshold (typically $\frac{S}{2}$), then one resamples. In our study, we use the resample algorithm in [26], i.e. Sample $u \sim \mathcal{U}_{[0, \frac{1}{S}]}$ and define a set of real number $\{U_j := u + \frac{j-1}{S}\}_{j=1, \dots, S}$. Then count the number of the set $\{U_j | \frac{\sum_{i=1}^{i'-1} w_t^{(i)}}{\sum_{i=1}^S w_t^{(i)}} \leq U_j \leq \frac{\sum_{i=1}^{i'} w_t^{(i)}}{\sum_{i=1}^S w_t^{(i)}}\}$ as the number of 'children' of sample $x^{(i')}$.

The essential of SMC methods is the design of importance densities, so that all samples have (almost) equal weights in each recursive step while staying on the trajectories with high likelihood. The algorithm based on a simple choice of $q(x_t | x_{1:t-1}, z_{1:t}) = p(x_t | x_{t-1})$, often referred as sequential importance sampling with resampling (SIR), performs poorly (see section section IV-C). Inspired by the ideas of implicit sampling (see Section III-C) and Auxiliary particle filtering, we propose to construct Gaussian importance densities by a combination of them (see Section III-C). To rejuvenate the samples, we will also introduce MCMC-move and information-move algorithms, which will be discussed in Section III-D and III-E, respectively.

B. Optimal one-step importance sampling

The one-step optimal importance density, which is the one-step posterior density that combines the prior from the state model and the likelihood of observation, is

$$q^{\text{opt}}(x_t | x_{1:t-1}, z_{1:t}) = \frac{p(z_t | x_t) \cdot p(x_t | x_{t-1})}{p(z_t | x_{t-1})}. \quad (11)$$

It is optimal in the sense that it leads to minimum variance in the incremental weights in (7). In general, it is difficult to draw samples from the optimal importance density and implicit sampling [15], [27] can efficiently draw samples in the high probability region. Thanks to the simple Gaussian structure of the noises ϵ_t and ξ_t in the state-space model (4), the optimal importance density is Gaussian and can be sampled directly. We can follow the procedure implicit sampling [15] to compute the mean and variance of the Gaussian posterior: the mean is the maximum a posteriori (MAP), and the variance is the Hessian of the negative logarithm of the posterior. More specifically, we compute the minimizer and Hessian of the negative log function of $p(z_t | x)p(x | x_{t-1})$:

$$F(x) = \frac{(z_t - Hx)^2}{2\xi_{0,t}^2} + \frac{(x - g(x_{t-1}))^2}{2\epsilon_{0,t}^2}.$$

This function is quadratic and its minimizer, denoted by $x_t^* = x^*(x_{t-1}, z_t) = [Hx_t^*, Gx_t^*]$, is:

$$\begin{cases} Hx_t^* = \frac{\epsilon_{0,t}^2 z_t + \xi_{0,t}^2 Hg(x_{t-1})}{\epsilon_{0,t}^2 + \xi_{0,t}^2} \\ = Hg(x_{t-1}) + \alpha_t(z_t - Hg(x_{t-1})), \\ Gx_t^* = Gg(x_{t-1}), \end{cases} \quad (12)$$

where $\alpha_t = \frac{(\xi_{0,t}/\epsilon_{0,t})^2}{(\xi_{0,t}/\epsilon_{0,t})^2 + 1}$ depends on the ratio between state-noise and observation-noise. The Hessian matrix of $F(x)$ is

$$\text{Hess}(F)_{i,j} = \begin{cases} \frac{1}{\xi_{0,t}^2} + \frac{1}{\epsilon_{0,t}^2}, & i = j \in \{1, \dots, N_1\}, \\ \frac{1}{\epsilon_{0,t}^2}, & i = j \in \{N_1 + 1, \dots, N\}, \\ 0, & \text{otherwise}, \end{cases} \quad (13)$$

Thus, the optimal importance density is Gaussian and can be sampled directly:

$$q(x_t | x_{1:t-1}, z_{1:t}) \sim \mathcal{N}(x_t^*, \text{Hess}(F)^{-1}) \quad (14)$$

with x_t^* in (12) and with $\text{Hess}(F)$ in (13).

The center x_t^* of the optimal importance density can be viewed as an effort of nudging solutions to the observation z_t . More generally, one can replace $\alpha_t(z_t - Hg(x_{t-1}))$ by a more general construction of the nudging term [20], [28]:

$$\lambda_t \mathbf{M}_t(z_t - Hg(x_{t-1})), \quad (15)$$

where $\lambda_t \in \mathbb{R}$ represents the nudging strength, and $\mathbf{M}_t \in \mathbb{R}^{dN \times dN_1}$ is called nudging matrix. Clearly, x_t^* can be put into this frame with a nudging matrix: $\mathbf{M}_t = [\mathbf{I}_{dN_1 \times dN_1}; \mathbf{0}_{dN_2 \times dN_1}]$ and $\lambda_t = \alpha_t$, optimal in the sense of maximizing the one-step posterior.

Though optimal for one-step sampling, the above importance density comes with drawbacks: the mean of the unobserved variables, $Gx_t^* = Gg(x_{t-1})$, is simply a projection of the forward equation from the previous state, without using any information from the current observation z_t . This can also be seen from the nudging matrix in (15), in which a block $\mathbf{0}_{dN_2 \times dN_1}$ does not provide any updates to the unobserved variables. Empirically, one may seek a nudging matrix that updates the unobserved variables to achieve better performance. Since the next observation z_{t+1} is a function of the current unobserved variables Gx_t , it is natural to update Gx_t using the information in z_{t+1} as in auxiliary particle filter [23].

C. Auxiliary sampling with two observations

The auxiliary particle filter is an SMC algorithm that makes use of the information from the next observation. To keep the recursive form as in (9), we need to consider target densities $p(x_{1:t} | z_{1:t+1})$ instead of $p(x_{1:t} | z_{1:t})$, and write it recursively as

$$\begin{aligned} p(x_{1:t} | z_{1:t+1}) &\propto p(x_{1:t-1} | z_{1:t}) \\ &\times \frac{p(x_t | x_{t-1})p(z_t | x_t)p(z_{t+1} | x_t)}{p(z_t | x_{t-1})}, \end{aligned}$$

Since the analytical expression of $p(z_{t+1} | x_t)$ is unknown, we approximate it by $p(z_{t+1} | x_t) \approx p(z_{t+1} | g(x_t))$ and obtain:

$$\begin{aligned} \hat{p}(x_{1:t} | z_{1:t+1}) &\propto \hat{p}(x_{1:t-1} | z_{1:t}) \\ &\times \frac{p(x_t | x_{t-1})p(z_t | x_t)p(z_{t+1} | g(x_t))}{p(z_t | g(x_{t-1}))}. \end{aligned} \quad (16)$$

With an importance density $q(x_t | x_{t-1}, z_{t:t+1})$ depending on z_{t+1} , the recursively updating weight becomes $w(x_{1:t} | z_{1:t+1}) = w(x_{1:t-1} | z_{1:t})\alpha(x_{t-1:t}, z_{t:t+1})$, where the associated incremental weight is given by:

$$\alpha(x_{t-1:t}, z_{t:t+1}) = \frac{p(x_t | x_{t-1})p(z_t | x_t)p(z_{t+1} | g(x_t))}{p(z_t | g(x_{t-1}))q(x_t | x_{t-1}, z_{t:t+1})}. \quad (17)$$

Next, we construct the importance density $q(x_t | x_{t-1}, z_{t:t+1})$ and draw samples from it. We start from the negative log function of the posterior distribution $p(z_{t+1} | g(x)p(x | x_{t-1})p(z_t | x))$:

$$\hat{F}(x) = \frac{|z_{t+1} - Hg(x)|^2}{2\xi_{0,t}^2} + \frac{|x - g(x_{t-1})|^2}{2\epsilon_{0,t}^2} + \frac{|z_t - Hx|^2}{2\xi_{0,t}^2}.$$

Since the state variable is high-dimensional and its components being indistinguishable agents, it is difficult and computationally costly to find the minimizer of \hat{F} , who is likely to have multi-modes. This rules out a direct application of implicit sampling. However, by a linear approximation of the nonlinear function $g(x_t)$, we can directly construct a Gaussian importance density $q(x_t | x_{t-1}, z_{t:t+1})$ as the previous section. We linearize $Hg(x)$ at x_t^* since it is the most likely position before the next observation:

$$Hg(x) \approx Hg(x_t^*) + \nabla Hg(x_t^*)^T(x - x_t^*),$$

where $\nabla Hg(x_t^*) \in \mathbb{R}^{dN \times dN_1}$ is the gradient of Hg . In practice, when the interaction function ϕ is piecewise constant, the approximation of ∇Hg is computed in follows:

$$\nabla Hg(x) \approx \mathbf{R}^{IH}(x) + \mathbf{L}^H(x) \in \mathbb{R}^{dN \times dN_1}, \quad (18)$$

where the block matrices $\mathbf{R}^{IH}(\cdot) \in \mathbb{R}^{dN \times dN_1}$ and $\mathbf{L}^H(\cdot) \in \mathbb{R}^{dN_1 \times dN_1}$ are composed by submatrices $\mathbf{R}_{i,j}^{IH}(\cdot)$ and $\mathbf{L}_{i,j}^H(\cdot) \in \mathbb{R}^{d \times d}$, respectively:

$$\begin{aligned} \mathbf{R}_{i,j}^{IH}(x) &= \frac{1}{N} \phi(\|x^i - H_j x\|) I_d, \\ \mathbf{L}_{i,j}^H(x) &= \begin{cases} -\frac{1}{N} \sum_{k=1}^N \phi(\|x^k - x^i\|) I_d, & \text{if } 1 \leq j = i \leq N_1, \\ 0 \times I_d, & \text{otherwise.} \end{cases} \end{aligned}$$

Then, $\hat{F}(x)$ can be approximated by a quadratic function:

$$\begin{aligned} \tilde{F}(x) &= \frac{|z_{t+1} - Hg(x_t^*) - \nabla Hg(x_t^*)^T(x - x_t^*)|^2}{2\xi_{0,t}^2} \\ &+ \frac{|x - g(x_{t-1})|^2}{2\epsilon_{0,t}^2} + \frac{|z_t - Hx|^2}{2\xi_{0,t}^2} \\ &= \frac{1}{2} y^T A y - y^T b + C \end{aligned}$$

with $y = x - x_t^*$, $C = \frac{|z_{t+1} - Hg(x_t^*)|^2}{2\xi_{0,t}^2} + \frac{|g(x_{t-1}) - x_t^*|^2}{2\epsilon_{0,t}^2} + \frac{|z_t - Hx_t^*|^2}{2\xi_{0,t}^2}$, and

$$\begin{cases} A = \frac{\nabla Hg(x_t^*) \nabla Hg(x_t^*)^T}{\xi_{0,t}^2} + \frac{I_N}{\epsilon_{0,t}^2} + \frac{H^T H}{\xi_{0,t}^2}, \\ b = \frac{\nabla Hg(x_t^*)^T [z_{t+1} - Hg(x_t^*)]}{\xi_{0,t}^2} + \frac{g(x_{t-1}) - x_t^*}{\epsilon_{0,t}^2} \\ \quad + \frac{H^T [z_t - Hx_t^*]}{\xi_{0,t}^2}. \end{cases} \quad (19)$$

Then, \tilde{F} has a minimizer $\mu(x_{t-1}, z_t, z_{t+1})$ given by:

$$\mu(x_{t-1}, z_t, z_{t+1}) = x_t^* + A^{-1}b \quad (20)$$

and its Hessian is A . This suggests the following importance density $q(x_t | x_{t-1}, z_t, z_{t+1})$:

$$q(x_t | x_{t-1}, z_t, z_{t+1}) \sim \mathcal{N}(\mu(x_{t-1}, z_t, z_{t+1}), A^{-1}), \quad (21)$$

where $\mu(x_{t-1}, z_t, z_{t+1})$ is defined by (20) and $A = A(x_{t-1}, z_t)$ is defined by (19).

We summarize the above in the following algorithm:

Algorithm 1 Auxiliary implicit sampling

At time $t \leq T - 1$, for $s = 1, 2, \dots, S$, do:

- Evaluate $x_t^* = x^*(x_{t-1}^{(s)}, z_t)$ as in (12), and then compute $A(x_{t-1}^{(s)}, z_t) = A$ as in (19) and $\mu(x_{t-1}^{(s)}, z_t, z_{t+1})$ as in (20).
- Draw a sample $x_t^{(s)}$ from a normal distribution with mean $\mu(x_{t-1}^{(s)}, z_t, z_{t+1})$ and covariance $A(x_{t-1}^{(s)}, z_t)^{-1}$; evaluate weights $\hat{w}_t^{(s)} = w_{t-1}^{(s)} \cdot \alpha_t^{(s)}$ as in (17).
- Resample to obtain equally-weighted samples (if a criterion is met).

At time $t = T$, for $s = 1, 2, \dots, S$, do Implicit sampling:

- Evaluate $x_t^* = x^*(x_{t-1}^{(s)}, z_t)$ as in (12).
 - Draw a sample $x_t^{(s)}$ from $\mathcal{N}(x_t^*, \text{Hess}(F)^{-1})$ as in (14); evaluate weights $\hat{w}_t^{(s)}$ by (10).
-

D. MCMC-move

To further reduce the inevitable degeneracy of SMC algorithms, we introduce an MCMC-move step [29]. We consider two types of moves: a directional move aiming for agent-wise position improvement, and a local trajectory move aiming to replace a low weight short-trajectory by a higher weighted one

The **directional move** randomly selects m of the unobserved agents for each sample, and resample each of them using a Metropolis-Hastings step as follows. For each selected agent k , first draw a sample from $\mathcal{N}(x_*^k, \Sigma_*^k)$, where x_*^k is a minimizer of the function

$$\tilde{g}(x_t^k | z_{t+1}, x_t^{1:k-1, k+1:N}) = \|z_{t+1} - Hg(x_t)\|^2,$$

and Σ_*^k is the Hessian of the function \tilde{g} at x_*^k , that is,

$$x_*^k = \arg \min_{x \in \mathbb{R}^d} \tilde{g}(x); \quad \Sigma_*^k = \text{Hess} \tilde{g}(x_*^k). \quad (22)$$

Then, accept the sample if it leads to a higher likelihood for observation z_t . The number m is chosen as $\lfloor \alpha N_2 \rfloor$ (we pick $\alpha = 0.2$). We summarize the directional move in Algorithm 2.

Algorithm 2 Directional move

At time $t \in \text{checking-time} \subset \{1, \dots, T\}$, for each sample, do:

- Randomly select $m = \lfloor 0.2N_2 \rfloor$ of the unobserved agents.
 - Move the selected agents: for $k = 1, \dots, N_2$, if the agent is among those selected, sample $\tilde{x}_t^k \sim \mathcal{N}(x_*^k, \Sigma_*^k)$, where x_*^k and Σ_*^k are defined in (22); else, set $\tilde{x}_t^k = x_t^k$.
 - Accept the move and set $x'_{1:t} = [x_{1:t-1}, \tilde{x}_t]$ if $u \sim \mathcal{U}_{[0,1]} \leq \min \left\{ 1, \frac{p(z_t | \tilde{x}_t)}{p(z_t | x_t)} \right\}$; otherwise, reject the move and set $x'_{1:t} = x_{1:t}$.
-

The **local trajectory move** randomly selects low-weighted samples and replaces their local trajectories by those with a higher probability. More precisely, at a prescribed time, a sample with index s is selected with probability $\max \left\{ 0, 1 - \frac{w_t^{(s)}}{c_t} \right\}$, where c_t is the value of the lowest quartile of the weights $\{w_t^{(s)}\}_{s=1}^S$. Intuitively speaking, all samples with weight higher than c_t will be kept and a sample with weight less than c_t will be selected randomly, according to a probability that increases when its weight decreases. Once selected, its local trajectory $x_{t-T_0:t}^{(s)}$ is moved to $\tilde{x}_{t-T_0:t}^{(s)}$ as in Algorithm 3.

Algorithm 3 Local-trajectory move

At time $t \in \text{checking-time} \subset \{1, \dots, T\}$, with samples $\{x_{1:t}^{(s)}, w_t^{(s)}\}_{s=1}^S$ and the weights $\{w_{t-T_0}^{(s)}\}_{s=1}^S$, do:

- Select low-weighted samples: for $s \in \{1, \dots, S\}$, set an indicator $\Theta_t^{(s)} = 1$ with probability $\max \left\{ 0, 1 - \frac{w_t^{(s)}}{c_t} \right\}$, where c_t is the value of the lowest quartile of the weights $\{w_t^{(s)}\}_{s=1}^S$;
 - Move the low-weighted samples: for $s \in \{1, \dots, S\}$, if $\Theta_t^{(s)} = 1$, replace the local trajectory $x_{t-T_0:t}^{(s)}$ by as follows:
 - Draw a sample $\tilde{x}_{t-T_0}^{(s)}$ from the samples $\{x_{t-T_0}^{(s)}, w_{t-T_0}^{(s)}\}_{s=1}^S$;
 - Implement a directional move for $\tilde{x}_{t-T_0}^{(s)}$ as in Algorithm 2, in which, draw new positions for m of the unobserved agents from the initial distribution, instead of drawing samples from $\mathcal{N}(x_*^k, \Sigma_*^k)$;
 - Draw $\tilde{x}_{t-T_0:t}^{(s)}$ by a one-sample SMC algorithm with importance density function in (21) from $t - T_0$ to t with initial value $\tilde{x}_{t-T_0}^{(s)}$;
 - Accept the move and set $x_{t-T_0:t}^{(s)} = \tilde{x}_{t-T_0:t}^{(s)}$, $w_t^{(s)} = c_t$ if $u \sim \mathcal{U}_{[0,1]} \leq \min \left\{ 1, \frac{p(z_t | \tilde{x}_t)}{p(z_t | x_t)} \right\}$; otherwise, reject the move and keep them as original.
-

E. Rejection of non-physical samples

To avoid non-physical samples, we introduce an **information move** step, rejecting non-physical samples. We say a sample is non-physical if it violates the basic properties of the opinion dynamics. For example, recall the following contraction of radius property of opinion dynamics [3, Proposition 2.1]: for any constant $c \in \mathbb{R}^d$, we have:

$$\max_i \|x_t^i - c\| \leq \max_i \|x_{t'}^i - c\|, \quad \forall t \geq t'.$$

This property requires information of all agents, and it can not be directly applied to our partial observations. Since the mean position of all agents does not change in time, we say a sample at time t is non-physical if

$$\max_i \|x_t^i - \bar{x}_{t-t_0}\| > \max_i \|x_{t'}^i - \bar{x}_{t-t_0}\| + \alpha, \quad \forall t \geq t'. \quad (23)$$

where t_0 and $\alpha > 0$ are constants (in practice, $t_0 = 10$ and $\alpha = 0.3 \times \text{supp}(\phi)$), representing the time length we back-track for checking and the tolerance for extending the maximal distance, respectively.

We also reject agents that do not interact with any of the observed agents. Such agents may be connected to the observed agents through other unobserved agents (recall that x_t^i and x_t^j are connected if there exists a path of agents $\{x_t^{i_k}\}_{k=0}^K$ with $i_0 = i$ and $i_K = j$ such that $\phi(\|x_t^{i_k} - x_t^{i_{k+1}}\|) > 0$), but their positions are difficult to estimate from the limited information. It is of interest to replace them by agents that interact with the observations: if they evolve to disconnect from the observed agents, their clustering can not be estimated from the observations, thus we can view them as “non-physical” (or with little information); otherwise, they will move toward the center of the cluster, and the replacement will accelerate their move.

In addition, to avoid over-correction and to maintain computational efficiency, we apply the rejection-moves at a pre-specified time steps that performed progressively less frequently as observation increases.

The information move algorithm is summarized in Algorithm 4:

Algorithm 4 Information move

For $t \in \text{checking-time} \subset \{1, \dots, T\}$ and for each sample, do:

- For $j = 1, \dots, N_2$, check if x_t is non-physical as in (23) or if it has agents disconnected from the observed agents. If yes, draw a sample \tilde{x}_t from the importance density in (21) and repeat until the sample is physical and connected with the observed agents.
 - If $u \sim \mathcal{U}_{[0,1]} \leq \min \left\{ 1, \frac{p(z_t | \tilde{x}_t)}{p(z_t | x_t)} \right\}$, set $x_t = \tilde{x}_t$; else, repeat from the previous step until accepted.
-

F. Summary

We combine all the above sampling techniques into Algorithm 5, which we refer it as auxiliary implicit sampling (AIS).

Algorithm 5 Auxiliary implicit sampling with MCMC moves (AIS)

At time $t = 1$, initialization: draw uniform-weighted samples $\{x_1^{(s)}, w_0^{(s)}\}$ from $\mu(x_1)$.

For time $t \geq 2$, do:

- Draw weighted sample $\{x_{1:t}^{(s)}, w_t^{(s)}\}$ by the Auxiliary implicit Sampling Algorithm 1.
 - Improve the samples by two MCMC moves: the Directional Move Algorithm 2 and the Local Trajectory Move Algorithm 3.
 - Reject non-physical samples by the Information Move Algorithm 4.
-

IV. NUMERICAL EXPERIMENTS

In this section, we predict the clustering of the opinion dynamics using partial observations, following the Bayesian approach discussed in Section II, using the auxiliary implicit sampling (AIS) algorithm introduced in Section III. We first describe the settings of the model and the sampling method in Section IV-A. Then, we present results on state estimation in Section IV-B. We report the prediction of clustering in a typical simulation in Section IV-C and in many simulations in Section IV-D.

A. Numerical settings

We consider the opinion dynamics (1) with $N = 60$ agents,

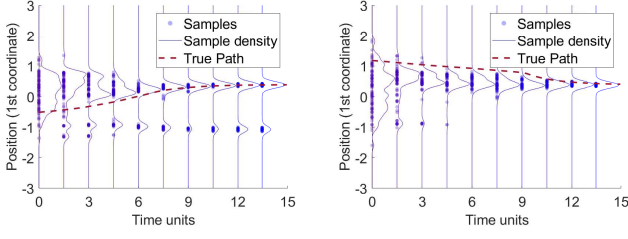
$$x_{t+1}^i - x_t^i = \frac{1}{N} \sum_{j=1}^N \phi(\|x_t^j - x_t^i\|)(x_t^j - x_t^i) \Delta t$$

where $x_t^i \in \mathbb{R}^d$ with $d = 2$ represents the opinion of the agent i at discrete times indexed by t . This system is an Euler approximation of the corresponding differential equations with time step size $\Delta t = 0.05$. The communication function ϕ is a piecewise-constant function:

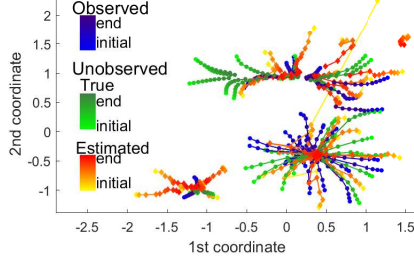
$$\phi(r) = \begin{cases} 1, & r \in [0, \sqrt{2}/2), \\ 0.1, & r \in [\sqrt{2}/2, 1), \\ 0, & r \in [1, \infty). \end{cases}$$

We are interested in the cases when the system formulates multiple clusters, instead of a consensus. For the above communication function, we obtain cases of multiple clusters by selecting the initial conditions as follows: we randomly draw initial condition for each agent from $\mu \sim \text{Unif}([-4, 4]^d)$, in other words, the initial distribution of (x_0^1, \dots, x_0^N) is $\mu^{\otimes N}$ on \mathbb{R}^{dN} , and reject those leading to consensus. We will call the empirical distribution of these selected initial conditions as initial distribution of the opinion dynamics. This initial distribution injects randomness into the dynamics.

Our goal is to predict the clustering of the system, particularly the sizes and the locations of the largest clusters, supposing that we only observe the trajectories of N_1 of the N agents for a relatively short time, far before the clusters are formulated. In particular, we assume that we observe the system for only $n = 300$ time steps, when the observations can not tell if the clusters have formulated. The clustering



(a) The 1st coordinate of two unobserved agents



(b) Trajectories of all agents: truth and a sample

Fig. 2: State estimation (noiseless observations): Estimation of the trajectory of agents for system without noise, observing $N_1 = 30$ of the $N = 60$ agents. (2a) shows the paths of the first coordinate of two unobserved agents for all the $S = 100$ samples (blue dots). At each time, the blue curve is the smoothed empirical density of the samples (sample density), representing the marginal posterior. For each agent, samples become concentrated around the truth (the red dash line) as time increases, with the marginal posterior peaks near the truth. (2b) shows the trajectories of all agents, where the blue and green dots are the observed and unobserved truth, and the red diamonds are the unobserved agents estimate by a sample; all with color changing from light to dark as time increases. The estimated trajectories of unobserved agents by the sample can be far away from the truth, particularly at the initial time, but the clustering of the sample is close to the truth.

usually takes more than 30 time units, or equivalently 600 time steps. (For instance, the system described by figure (4) clustered at about 1500 time steps.) As discussed in Section II, a Bayesian approach provides a probabilistic framework for state estimation and cluster prediction, with uncertainties quantified by the posterior. We sample the posterior by the auxiliary implicit sampling (AIS) algorithm in Algorithm 5 with ensemble size $S = 100$. For the sake of the AIS, we rewrite the system in the form of a state-space model:

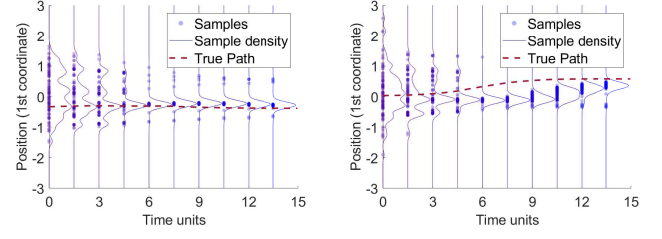
$$\begin{cases} x_{t+1} = g(x_t) + \epsilon_t, & x_1^i \sim \mu, \forall i, \\ z_t = Hx_t + \xi_t, \end{cases}$$

where $\epsilon_t \sim \mathcal{N}(0, \alpha^2 I_{dN})$; $\xi_t \sim \mathcal{N}(0, \beta^2 I_{dN_1})$.

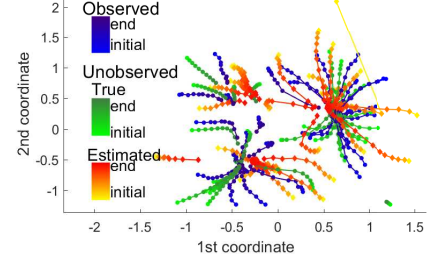
We consider systems with both noiseless and noisy observations. To avoid degenerate distributions, we set an artificial noise for the deterministic state model. For the case of noiseless observations, we set $\alpha = 10^{-4}$ and $\beta = \frac{1}{4}10^{-4}$. For noisy observations with $\beta = 0.01$ (which represents a signal-to-noise ratio about 1% -2%,), we set $\alpha = 0.05$.

B. State estimation

As a Bayesian approach, our goal of state estimation is to represent the posterior of the states, which is approximated by the empirical measure of the samples in our sequential Monte Carlo algorithm. We demonstrate the state estimation by the marginal posteriors of the trajectories of the first coordinate



(a) The 1st coordinate of two unobserved agents



(b) Trajectories of all agents: truth and a sample

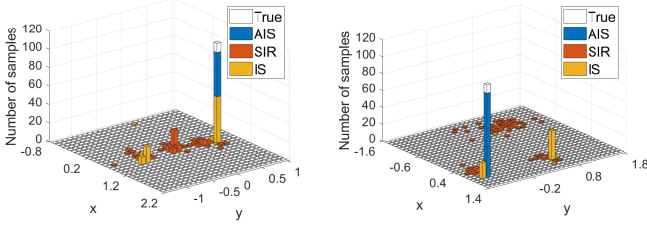
Fig. 3: State estimation (noisy observations): Estimation of the trajectory of agents when observing $N_1 = 30$ of the $N = 60$ agents with additive Gaussian noise. In (3a), the samples (blue dots) of the 1st coordinate become concentrated around the truth (the red dash line) as time increases, with the multi-mode sample density (blue line) peaks near the truth. (3b) shows the trajectories of all agents, where the blue and green dots are the observed and unobserved truth, and the red diamonds are the unobserved agents estimated by a sample; all with color changing from light to dark as time increases. The estimated trajectories of unobserved agents by the sample can be far away from the truth, particularly at the initial time, but the clustering of the sample is close to the truth.

of two unobserved agents. We also show the trajectories of all agents, comparing the estimated path of unobserved agents in a sample with the truth.

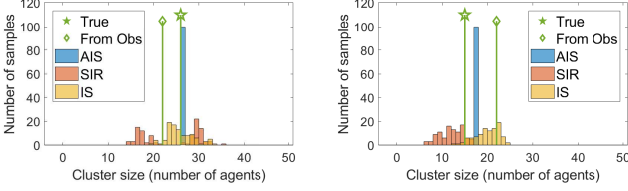
a) Noiseless observations: Consider first the case when the system is deterministic and half of the $N = 60$ agents are observed without noise. Figure (2a) shows the trajectories of all the $S = 100$ samples for the first coordinate of two unobserved agents, along with the smoothed sample density at each time, representing the marginal posterior. For each agent, samples become concentrated around the truth (the red dash line) as time increases, with the marginal posterior peaks near the truth. Such a concentration of the sample agrees with the intuition that the uncertainty in the posterior of the states decreases when more observations are available, since the system is deterministic and the randomness comes only from the initial condition. The marginal posterior has multiple modes, reflecting the symmetry between agents and the non-identifiability of the states as discussed in Section II-C.

Figure (2b) shows the trajectories of all agents, comparing the estimated paths of unobserved agents estimated by a sample with the truth. The estimated trajectories by the sample can be far away from the truth, particularly at the initial time, but the clustering of the sample is close to the truth.

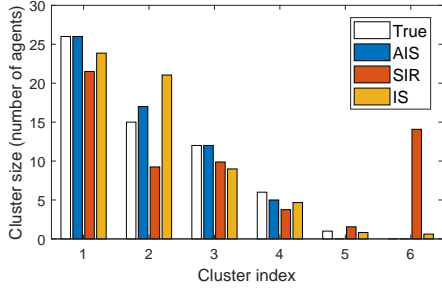
b) Noisy observations: We also consider the case when half of the $N = 60$ agents are observed with additive Gaussian noise $\mathcal{N}(0, \beta^2 I_{dN_1})$. Similarly, Figure (3a) shows the trajectories of all the $S = 100$ samples for the first coordinate of two unobserved agents, along with the smoothed empirical sample



(a) Posterior of cluster center: the largest (left) and 2nd largest (right) cluster

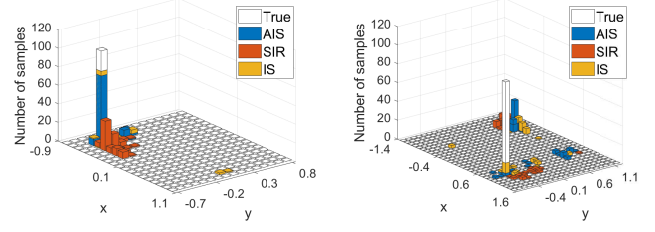


(b) Posterior of cluster size: the largest (left) and 2nd largest (right) cluster

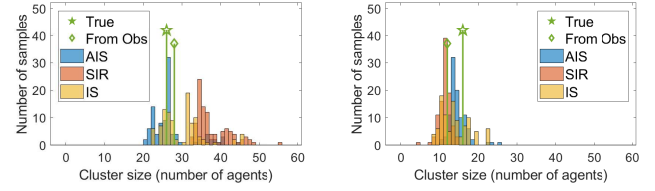


(c) Sizes of all clusters (estimated by sample mean)

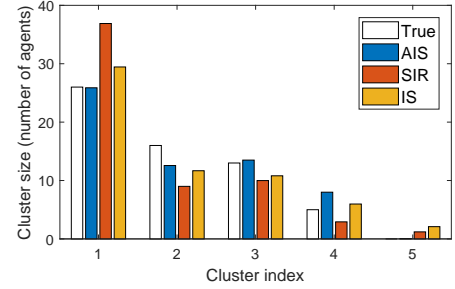
Fig. 4: Clustering prediction (noiseless observations): prediction of centers and sizes of clusters when observing $N_1 = 30$ of the $N = 60$ agents for a short time. AIS algorithm outperforms SIR and IS at presenting concentrations around the truth posteriors of the centers and sizes for the leading clusters, and at providing accurate estimation of sizes for all clusters by sample mean.



(a) Posterior of cluster center: the largest (left) and 2nd largest (right) cluster



(b) Posterior of cluster size: the largest (left) and 2nd largest (right) cluster



(c) Sizes of all clusters (estimated by sample mean)

Fig. 5: Clustering prediction (noisy observations): prediction of centers and sizes of clusters when observing $N_1 = 30$ of the $N = 60$ agents for a short time with additive Gaussian noise. AIS algorithm performs slightly better than IS and clearly outperforms SIR, at presenting posteriors of the centers and sizes for the leading clusters, and at providing accurate estimation of sizes for all clusters by sample mean.

density at each time, representing the marginal posterior. For each agent, the sample density is more wide-spread and has more modes than those in Figure 2 for the deterministic system, indicating more uncertainty due to the noises in the system and in the observation. But all samples become concentrated around the truth eventually as time increases, with the marginal posterior peaks near the truth.

Figure (3b) shows the trajectories of all agents, comparing the estimated paths of unobserved agents estimated by a sample with the truth. Again, the estimated trajectories by the sample can be far away from the truth, particularly at the initial time, but the clustering of the sample is close to the truth.

In summary, in both noiseless and noisy observations, the marginal posteriors of the state can be multi-mode, presenting a large uncertainty; the trajectories of the samples can be far from the truth, but the clustering pattern of the samples is close to the truth.

C. Clustering prediction: a typical simulation

In this and the next section, we consider the prediction of clusters from partial observations. We exhibit the cluster prediction of a typical simulation in this section, and we report the performance in many simulations in the next section.

Recall that in a typical clustering prediction, we characterize the clustering by the posteriors of the sizes and centers of the

clusters, particularly the leading clusters. We compare our AIS algorithm with two other SMC algorithms: SIR and implicit sampling (denoted by IS). Since the degeneracy of samples in SIR is too severe for any meaningful prediction, we reduce the degeneracy by inflating its weights to keep more samples in each step. For the prediction of the sizes, we also compare AIS with the predictions simply based on connected agents from observation x_T only, since in practice one may treat the observation as a random sample of the population.

a) Noiseless observations. Figure (4a)–(4b) show the empirical posteriors of the centers and sizes for the largest cluster and the second largest cluster (defined in Eq.(5)). Consider first the centers of the clusters in Figure (4a). The true center of the largest cluster locates at the white bar in the left plot. All samples from AIS are close to the true center (with a distance less than 0.1, resulting in a bar overlapping with the white bar of the true center). IS has about half samples at the true center and the other half far away from the true center. Nearly all samples of SIR mispredicted the true center. Similar results can be seen in the right plot.

Consider next the cluster sizes in Figure (4b). The largest cluster has 27 agents, and the second largest cluster has 18 agents. The predicted sizes based on the observation x_T only (denoted by “From Obs”) are both 22, not being able to

identify the leading clusters. This suggests that the observation x_T itself is not enough to make an accurate prediction of the clustering. Among the SMC algorithms, AIS leads to highly concentrated samples, at the true size for the largest cluster and near the true size for the second largest cluster. Implicit sampling (IS) leads to samples scattering around the truth. The samples of SIR scatter widely, tending to overestimate the size of the largest cluster and underestimate the size of the second largest cluster.

Since the system is deterministic and the observations are noiseless, the true posterior of concentrates around the truth. AIS outperforms SIR and IS at representing such concentrated posterior.

Figure (4c) shows the sizes of all the clusters, estimated by sample mean as in (6). AIS accurately captures the sizes of all the clusters except the smallest one, which is too small to be predicted. IS performed relatively well in predicting the largest cluster, but misses the 2nd largest cluster. SIR identifies the largest cluster with a relatively large error (5 relative to 27), but it misses all the other clusters.

b) Noisy observations: Figure 5 shows the predictions when the observations are noisy. Due to the observation noise, the posteriors of the centers and sizes would present a larger uncertainty than the case of noiseless observations. Figure (5a) shows the posteriors of centers for the two largest clusters. For the largest cluster, all three SMC algorithms yield samples scatter close to the true centers, with samples of AIS and IS concentrating at the true center more than those of SIR. For the second largest cluster, an unusual result appears: all the SMC algorithms lead to samples mostly missing the position of the true center. The reason is that the second and the third largest clusters have similar sizes (as shown in Figure (5c), the sizes are 16 and 13, respectively), causing difficulty in distinguishing them.

Figure (5b) presents posteriors of the sizes for the two largest clusters. The largest cluster has 26 agents, and the second largest cluster has 16 agents. AIS leads to samples concentrating at the true size for the largest cluster and near the true size for the second largest cluster. IS leads to samples scattering slightly wider than AIS, but are still around the truth. The samples of SIR scatter widely, tending to overestimate the size of the largest cluster and underestimate the size of the second largest cluster. The predicted sizes based on the observation x_T only (denoted by “From Obs”) are 28 and 12, slightly overestimating the size of the largest cluster and underestimating the size of the second largest cluster.

Figure (5c) shows the sizes of all the clusters, estimated by sample mean as in (6). Only AIS accurately captures the size of the largest cluster, IS slightly overestimates the size, and SIR has an estimation that is too large. All three algorithms are able to lead to similar sizes for the second and the third clusters, with AIS being the closest to the truth. Note that all the SMC algorithms predict an untrue fifth cluster, but AIS has the smallest error.

In summary, for predicting centers and sizes of clusters from either noiseless or noisy observations, the performance of AIS algorithm is much better than that of SIR, which is usually

not satisfactory, and is better than that of IS, which is often reasonably good.

D. Clustering prediction: success rates in many simulations

We further investigate the clustering prediction by Auxiliary Implicit Sampling (AIS) in 100 independent simulations. We consider three cases: observing $\frac{1}{2}$, $\frac{1}{3}$, and $\frac{1}{6}$ of the 60 agents. We assess the performance by studying the success rate in predicting the centers for the largest two clusters, and the distribution of errors in size estimation.

a) Assessment of the prediction performance: Recall that we estimate the centers and sizes of clusters by their posterior means. More precisely, the center \bar{x}_{C_i} and size $|\widehat{C}_i|$ of cluster C_i are estimated by their sample means $\widehat{\bar{x}}_{C_i}$ and $|\widehat{C}_i|$ as defined by (6). We denote by C_1 and C_2 the largest and the second largest clusters.

For each simulation, we say the center of the largest cluster C_1 is predicted successfully if there exists an estimated cluster with a size in $[|C_1| - K, |C_1| + K]$ and with a center such that $\text{dist}(\bar{x}_{C_1}, \bar{x}_{C_j}) < L$. Here K and L are the levels of error tolerance. More specifically, we define an indicator function for a successful prediction of C_1 by

$$\Omega_1 = \begin{cases} 1, & \text{if } \text{dist}(\bar{x}_{C_1}, \widehat{\bar{x}}_{C_j}) \leq L \text{ for some } j \text{ such that} \\ & |C_1| - K < |\widehat{C}_j| < |C_1| + K; \\ 0, & \text{otherwise,} \end{cases} \quad (24)$$

In following simulations, we pick $L = 0.1$ (in general L should depend on the communication function ϕ , recall that our ϕ is supported in $[0, 1]$) and the range of the value $K \in \{0, 1, 2\}$. Similarly, we define a successful prediction for the center of the second largest cluster and its indicator function Ω_2 .

We access the prediction of the sizes of the largest two clusters by the distribution of the absolute error:

$$e_i = \left| |\widehat{C}_i^0| - |\widehat{C}_i| \right|, \text{ for } i = 1, 2. \quad (25)$$

The error e_i should be close to zero in a successful prediction. A heavy tail in the distribution of e_i would indicate that it is difficult to predict the cluster size accurately.

b) Noiseless observations: Figure 6 illustrates the performance of prediction of the largest two clusters in 100 independent simulations. We consider three observation ratios: $\frac{1}{2}$, $\frac{1}{3}$, or $\frac{1}{6}$, that is, observing 30, 20 and 10 of the $N = 60$ agents in the system. The distributions of errors in the estimation of cluster sizes are shown in Figure (6a)-(6b), and the success rate in predicting the centers are shown in Figure (6c)-(6d).

The prediction of cluster sizes depends on the observation ratio. When observing $\frac{1}{2}$ or $\frac{1}{3}$ of all agents, the majority simulations (more than 70%) can predict the cluster sizes with an error within 4. But when the observation ratio is $\frac{1}{6}$, many simulations have large errors (larger than 4 for more than 50% of the simulations), suggesting that the observations do not provide enough information for accurate prediction of the cluster sizes.

The prediction of cluster centers exhibits a high success rate, regardless of the observation ratio. Figure (6c)-(6d) show that

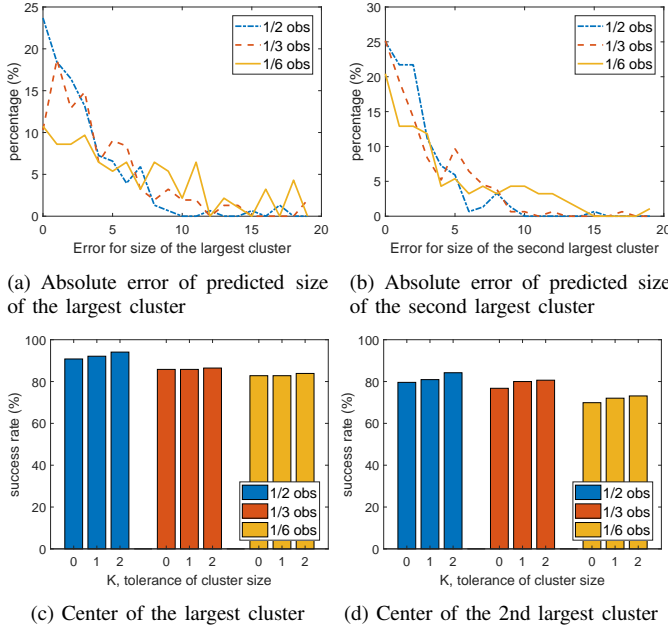


Fig. 6: Cluster prediction in 100 simulations (noiseless case): observing $\frac{1}{2}$, $\frac{1}{3}$, or $\frac{1}{6}$ of the $N = 60$ agents in the system. In (6a)-(6b), the majority simulations (more than 70%) can predict the cluster sizes reasonably, holding an error within 4, when the observation ratio is either $\frac{1}{2}$ or $\frac{1}{3}$; but when the observation ratio is $\frac{1}{6}$, many simulations have large errors. Figure (6c)-(6d) show that the centers of the leading clusters can be located with high probability (85%-95% for the largest cluster and 75%-85% for the second largest cluster) even only observing $\frac{1}{6}$ of all agents. The success rate depends little on the tolerance level K . In short, the observation ratio affects the prediction of cluster sizes, but not the cluster centers.

the centers of the leading clusters can be located with high probability 85%-95% for the largest cluster and 75%-85% for the second largest cluster, and that the success rate drops slightly when the observation ratio decreases from $\frac{1}{2}$ to $\frac{1}{6}$. Also, the success rate depends little on the tolerance level K .

c) Noisy observations: When the trajectories are observed with additive Gaussian noise, similar to the case of noiseless observations, the prediction for sizes is more sensitive to observation ratio than the prediction for centers. Due to the additional uncertainty from the observation noise, the error for size estimation is larger than the noiseless case. In (7a)-(7b), when the observation ratio is $\frac{1}{2}$ or $\frac{1}{3}$, about 70% of the simulations hold an error size less than 6; when the observation ratio is $\frac{1}{6}$, about 50% of the simulations have errors larger than 4. In particular, the size of the second largest cluster is predicted more accurately than the largest cluster, indicating that the observation noise is mostly absorbed in the prediction of the leading cluster.

The observation noise also slightly reduces the success rate in the prediction of cluster centers. In (7c)-(7d), the centers are predicted with a probability (around 85% and 80% for the largest and the second largest clusters, respectively), regardless of the observation ratio.

In summary, for either noiseless or noisy observations, the cluster center can be predicted with a high success rate, regardless of the observation ratio. The cluster size, on the other hand, has a larger uncertainty that is sensitive to the observation noise or the ratio of observation.

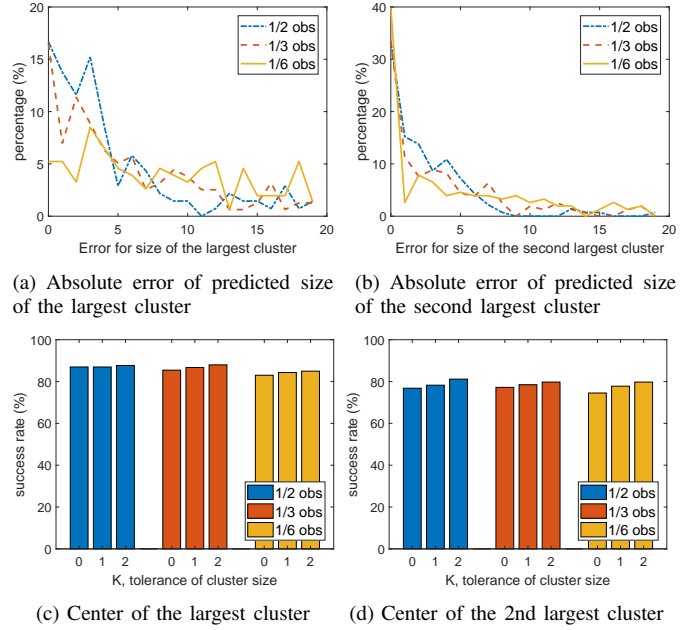


Fig. 7: Cluster prediction in 100 simulations (noisy observations), observing $\frac{1}{2}$, $\frac{1}{3}$, or $\frac{1}{6}$ of the $N = 60$ agents in the system with additive Gaussian noise. Similar to the case of noiseless observations: the prediction for sizes is more sensitive to observation ratio than the prediction of centers. In (7a)-(7b), the error for size estimation is relatively large: when the observation ratio is $\frac{1}{2}$ or $\frac{1}{3}$, about 70% of the simulations hold an error size less than 6; when the observation ratio is $\frac{1}{6}$, many simulations have large errors. In (7c)-(7d), the centers are predicted with a probability (around 85% and 80% for the largest and the second largest clusters, respectively), regardless of the observation ratio.

V. DISCUSSION AND CONCLUSION

We presented a Bayesian formulation for clustering prediction of opinion dynamics from partial observations, characterizing the prediction by the posterior of the clusters' sizes and centers. To overcome the challenge in sampling the high-dimensional posterior with multiple local maxima, we introduced an auxiliary implicit sampling (AIS) algorithm using two-step observations, which is a sequential Monte Carlo method that combines the ideas from auxiliary particle filters [23] and implicit particle filters [15]. In both cases of noiseless and noisy observations, the AIS algorithm leads to accurate predictions of the sizes and centers for the leading clusters. We found that uncertainty increases when the ratio of the observed population decreases. Also, the cluster center can be predicted with a high success rate, but the cluster size, on the other hand, has a more considerable uncertainty that is sensitive to the observation noise or the ratio of observation.

There are three directions for future research. First, improve the information in observation by a random selection of agents to be observed at each time. The observations in this study are trajectories of a fixed set of agents, which may yield little information about other clusters when these agents concentrate in one cluster. Random selection of agents may avoid such an information loss by providing an unbiased sampling of all the agents' opinions. Second, improve the scalability of the proposed techniques when the number of agents is large. One may describe the concentration density of the opinions by the mean-field equation [30] and apply

sequential Monte Carlo methods for the mean-field equation [22] or use reduced models [31], [32] to achieve efficiency. Third, learn the communication function [9], [10] along with network topology [33], as well as clustering prediction, from partial observations.

ACKNOWLEDGMENT

The authors would like to thank Mauro Maggioni and Sui Tang for inspiring discussions. The authors are grateful for supports from NSF-1913243, NSF-1821211, MARCC, and Johns Hopkins University.

REFERENCES

- [1] U. Krause, "A discrete nonlinear and non-autonomous model of consensus formation," *Communications in difference equations*, vol. 2000, pp. 227–236, 2000.
- [2] T. Vicsek and A. Zafeiris, "Collective motion," *Physics Reports*, vol. 517, pp. 71 – 140, 2012.
- [3] S. Motsch and E. Tadmor, "Heterophilous dynamics enhances consensus," *SIAM review*, vol. 56, no. 4, pp. 577–621, 2014.
- [4] J. Shao, S. Havlin, and H. E. Stanley, "Dynamic Opinion Model and Invasion Percolation," *Phys. Rev. Lett.*, vol. 103, no. 1, p. 018701, 2009.
- [5] Q. Li, L. A. Braunstein, H. Wang, J. Shao, H. E. Stanley, and S. Havlin, "Non-consensus Opinion Models on Complex Networks," *J Stat Phys*, vol. 151, no. 1-2, pp. 92–112, 2013.
- [6] A. V. Proskurnikov, A. S. Matveev, and M. Cao, "Opinion Dynamics in Social Networks With Hostile Camps: Consensus vs. Polarization," *IEEE Trans. Automat. Contr.*, vol. 61, no. 6, pp. 1524–1536, 2016.
- [7] A. Lancichinetti and S. Fortunato, "Consensus clustering in complex networks," *Sci Rep*, vol. 2, no. 1, p. 336, 2012.
- [8] M. Bongini, M. Fornasier, M. Hansen, and M. Maggioni, "Inferring interaction rules from observations of evolutive systems I: The variational approach," *Math. Models Methods Appl. Sci.*, vol. 27, no. 05, pp. 909–951, 2017.
- [9] F. Lu, M. Zhong, S. Tang, and M. Maggioni, "Nonparametric inference of interaction laws in systems of agents from trajectory data," *Proc Natl Acad Sci USA*, vol. 116, no. 29, pp. 14 424–14 433, 2019.
- [10] F. Lu, M. Maggioni, and S. Tang, "Learning interaction kernels in heterogeneous systems of agents from multiple trajectories," *arXiv preprint arXiv:1910.04832*, 2019.
- [11] M. Tucsnak and G. Weiss, *Observation and control for operator semigroups*. Springer Science & Business Media, 2009.
- [12] A. Doucet and A. M. Johansen, "A tutorial on particle filtering and smoothing: Fifteen years later," *Handbook of nonlinear filtering*, vol. 12, no. 656-704, p. 3, 2009.
- [13] W. R. Gilks and C. Berzuini, "Following a moving target Monte Carlo inference for dynamic Bayesian models," *Journal of the Royal Statistical Society: Series B (Statistical Methodology)*, vol. 63, no. 1, pp. 127–146, 2001.
- [14] C. Berzuini and W. Gilks, "Resample-move filtering with cross-model jumps," in *Sequential Monte Carlo Methods in Practice*. Springer, 2001, pp. 117–138.
- [15] A. J. Chorin and X. Tu, "Implicit sampling for particle filters," *Proc. Natl. Acad. Sci. USA*, vol. 106, no. 41, pp. 17 249–17 254, 2009.
- [16] E. Lunasin and E. S. Titi, "Finite determining parameters feedback control for distributed nonlinear dissipative systems - a computational study," *ArXiv150603709 Math*, 2017.
- [17] C. Foias, C. F. Mondaini, and E. S. Titi, "A discrete data assimilation scheme for the solutions of the 2D Navier-Stokes equations and their statistics," *ArXiv160205995 Math*, 2016.
- [18] X. Liu, W. Yu, J. Cao, and S. Chen, "Discontinuous lyapunov approach to state estimation and filtering of jumped systems with sampled-data," *Neural Networks*, vol. 68, pp. 12–22, 2015.
- [19] H. Nijmeijer, "A dynamical control view on synchronization," *Physica D: Nonlinear Phenomena*, vol. 154, no. 3-4, pp. 219–228, 2001.
- [20] D. Auroux and J. Blum, "Back and forth nudging algorithm for data assimilation problems," *Comptes Rendus Mathematique*, vol. 340, no. 12, pp. 873–878, 2005.
- [21] M. Zhu, P. J. Van Leeuwen, and J. Amezcu, "Implicit equal-weights particle filter," *Quarterly Journal of the Royal Meteorological Society*, vol. 142, no. 698, pp. 1904–1919, 2016.
- [22] F. Lu, N. Weitzel, and A. Monahan, "Joint state-parameter estimation of a nonlinear spde model from sparse noisy data," *preprint*, 2019.
- [23] M. K. Pitt and N. Shephard, "Filtering via simulation: Auxiliary particle filters," *Journal of the American statistical association*, vol. 94, no. 446, pp. 590–599, 1999.
- [24] A. Kong, J. S. Liu, and W. H. Wong, "Sequential imputations and bayesian missing data problems," *Journal of the American statistical association*, vol. 89, no. 425, pp. 278–288, 1994.
- [25] J. S. Liu, *Monte Carlo strategies in scientific computing*. Springer Science & Business Media, 2008.
- [26] G. Kitagawa, "Monte carlo filter and smoother for non-gaussian non-linear state space models," *Journal of computational and graphical statistics*, vol. 5, no. 1, pp. 1–25, 1996.
- [27] M. Morzfeld, X. Tu, J. Wilkening, and A. Chorin, "Parameter estimation by implicit sampling," *Communications in Applied Mathematics and Computational Science*, vol. 10, no. 2, pp. 205–225, 2015.
- [28] C. Paniconi, M. Marrocu, M. Putti, and M. Verbunt, "Newtonian nudging for a richards equation-based distributed hydrological model," *Advances in Water Resources*, vol. 26, no. 2, pp. 161–178, 2003.
- [29] C. Berzuini, N. G. Best, W. R. Gilks, and C. Larizza, "Dynamic conditional independence models and markov chain monte carlo methods," *Journal of the American Statistical Association*, vol. 92, no. 440, pp. 1403–1412, 1997.
- [30] P.-E. Jabin and J. C. Lagarias, "A review of the mean field limits for Vlasov equations," *Kinet. Relat. Models*, vol. 7, no. 4, pp. 661–711, 2014.
- [31] A. J. Chorin, F. Lu, R. M. Miller, M. Morzfeld, and X. Tu, "Sampling, feasibility, and priors in data assimilation," *Discrete Contin. Dyn. Syst. A*, vol. 36, no. 8, pp. 4227–4246, 2016.
- [32] F. Lu, X. Tu, and A. J. Chorin, "Accounting for model error from unresolved scales in ensemble kalman filters by stochastic parameterization," *Mon. Wea. Rev.*, vol. 145, no. 9, pp. 3709–3723, 2017.
- [33] M. Coutino, E. Isufi, T. Maehara, and G. Leus, "State-Space Network Topology Identification From Partial Observations," *IEEE Trans. on Signal and Inf. Process. over Networks*, vol. 6, pp. 211–225, 2020.